A Hybrid Representation of the Green's Function in an Overmoded Rectangular Cavity

DORIS I. WU, MEMBER, IEEE, AND DAVID C. CHANG, FELLOW, IEEE

Abstract—**A hybrid ray–mode representation of the Green's function in a rectangular cavity is developed using the finite Poisson summation formula. In order to obtain a numerically efficient scheme for computing the field generated by a point source in a large rectangular cavity, the conventional modal representation of the Green's function is modified in such a way that all the modes near resonance are retained while the truncated remainder of the mode series is expressed in terms of a weighted contribution of rays. For an electrically large cavity, the contribution of rays from distant images becomes small; therefore the ray sum can be approximated by one or two dominant terms without a loss of numerical accuracy. To illustrate the accuracy and the computational simplification of this ray–mode representation, numerical examples are included with the conventional mode series (summed at the expense of long computation time) serving as a reference.**

I. Introduction

In analyzing fields due to scattering or excitation of a radiating structure inside an electrically large and overmoded rectangular cavity such as the NBS reverberating chamber used in EMI testing [1], [2], we often encounter the dyadic Green's function expressed in the modal form as the kernel for the desired integral equation. One issue that often arises is how to obtain a numerically efficient scheme for computing the dyad, particularly when the observation point is close to the source point. A modal representation is clearly not practical, since the convergence of the triply infinite sum of higher order, nonresonant modes is notoriously, if not impractically, slow.

In this paper, a finite, three-dimensional Poisson summation formula is used to obtain a hybrid representation for the Green's function. This hybrid representation consists of two terms. The first term, called the mode sum, consists of a finite number of modes near resonance. The number of modes varies depending upon the bandwidth chosen. The second term, referred to as the ray sum, consists of all the images produced by the reflecting boundaries of the cavity. The bandwidth for the mode sum is a mathematical quantity. A balancing effect exists between the two terms in that as the bandwidth increases, the contribution from the mode sum increases while the contribution from the ray sum decreases. Though the bandwidth is an arbitrary quantity, it does have a minimal requirement. Below this minimal value the hybrid representation becomes a poor approximation to the modal representation. As will be shown, this minimal requirement stems from the approximation involved in transforming from the rectangular coordinates to spherical coordinates in applying the finite Poisson summation formulation.

The hybrid representation is especially effective when the source point is close to the observation point. For an electrically large cavity, often the second or the third layer images and beyond are far away from the observation point, so the contribution from these images becomes very small. Therefore, we have found that it is often sufficient to keep just the self term and perhaps several adjacent images for the ray sum to obtain the desired numerical accuracy.

Manuscript received December 11, 1987; revised April 12, 1988.

D. I. Wu is with the Electromagnetic Fields Division of the National Bureau of Standards, Boulder, CO 80303.

D. C. Chang is with the Department of Electrical and Computer Engineering, University of Colorado, Boulder, CO 80309.

IEEE Log Number 8822322.

II. Dyadic Green's Function

A complete dyadic Green's function of the electric type valid inside and outside of the source region in a rectangular cavity requires that it satisfies the appropriate boundary conditions on the cavity walls as well as the differential equation

$$\nabla \times \nabla \times \overleftrightarrow{G} - k_0^2 \overleftrightarrow{G} = \overleftrightarrow{I}\delta(r - r'), \qquad \overleftrightarrow{I} = \hat{x}\hat{x} + \hat{y}\hat{y} + \hat{z}\hat{z} \quad (1)$$

where k_0 is the free space wavenumber, r and r' represent the distances from the origin to the observation and the source point, respectively, and an $e^{j\omega t}$ time variation is assumed. As illustrated in [3] and [4], the solution to (1) can be represented in many ways. For example, one way to represent the dyad is to separate the field into a zero-divergence type, denoted by $\vec{E}^{te}$ and $\vec{E}^{tm}$, and a zero-curl type, denoted by $\vec{F}$, as

$$\overleftrightarrow{G} = \sum_{\alpha=(m,n,p)=0}^{\infty}\sum\sum\left[\frac{\vec{E}_\alpha^{te}(r)\vec{E}_\alpha^{te}(r')}{(k_\alpha^2 - k_0^2)k_{mn}^2} + \frac{\vec{E}_\alpha^{tm}(r)\vec{E}_\alpha^{tm}(r')}{(k_\alpha^2 - k_0^2)k_{mn}^2 k_\alpha^2} - \frac{\vec{F}_\alpha(r)\vec{F}_\alpha(r')}{k_\alpha^2 k_0^2}\right] \quad (2)$$

0018-9480/88/0900-1334$01.00 ©1988 IEEE

where

$$\vec{E}_\alpha^{\,te} = \nabla \times \frac{\epsilon_\alpha}{\sqrt{abc}} \cos\left(\frac{m\pi}{a}x\right)\cos\left(\frac{n\pi}{b}y\right)\sin\left(\frac{p\pi}{c}z\right)\hat{z}$$

$$\vec{E}_\alpha^{\,tm} = \nabla \times \nabla \times \frac{\epsilon_\alpha}{\sqrt{abc}} \sin\left(\frac{m\pi}{a}x\right)\sin\left(\frac{n\pi}{b}y\right)\cos\left(\frac{p\pi}{c}z\right)\hat{z}$$

$$\vec{F}_\alpha = \nabla\left(\frac{\epsilon_\alpha}{\sqrt{abc}} \sin\left(\frac{m\pi}{a}x\right)\sin\left(\frac{n\pi}{b}y\right)\sin\left(\frac{p\pi}{c}z\right)\right)$$

and

$$k_\alpha^2 = \left(\frac{m\pi}{a}\right)^2 + \left(\frac{n\pi}{b}\right)^2 + \left(\frac{p\pi}{c}\right)^2$$

$$k_{mn}^2 = \left(\frac{m\pi}{a}\right)^2 + \left(\frac{n\pi}{b}\right)^2$$

$$\epsilon_\alpha = \begin{cases} 2 & \text{for } m = 0, \text{ or } n = 0, \text{ or } p = 0 \\ \sqrt{8} & \text{for } m, n, p \neq 0. \end{cases}$$

Equation (2) for $\overleftrightarrow{G}$ can also be written in a different form using a set of modal functions similar to those used in waveguide theory. These modal functions are

$$\phi_\alpha^x(r) = \frac{\epsilon_\alpha}{\sqrt{abc}} \cos\left(\frac{m\pi}{a}x\right)\sin\left(\frac{n\pi}{b}y\right)\sin\left(\frac{p\pi}{c}z\right)$$

$$\phi_\alpha^y(r) = \frac{\epsilon_\alpha}{\sqrt{abc}} \sin\left(\frac{m\pi}{a}x\right)\cos\left(\frac{n\pi}{b}y\right)\sin\left(\frac{p\pi}{c}z\right)$$

$$\phi_\alpha^z(r) = \frac{\epsilon_\alpha}{\sqrt{abc}} \sin\left(\frac{m\pi}{a}x\right)\sin\left(\frac{n\pi}{b}y\right)\cos\left(\frac{p\pi}{c}z\right)$$

and

$$\Phi_\alpha(r) = \frac{\epsilon_\alpha}{\sqrt{abc}} \sin\left(\frac{m\pi}{a}x\right)\sin\left(\frac{n\pi}{b}y\right)\sin\left(\frac{p\pi}{c}z\right).$$

In terms of these modal functions, (2) can be written as

$$\overleftrightarrow{G} = -\nabla\nabla'\frac{1}{k_0^2}\sum\sum\sum_\alpha \frac{\Phi_\alpha(r)\Phi_\alpha(r')}{k_\alpha^2 - k_0^2} + \sum\sum\sum_\alpha \frac{1}{k_\alpha^2 - k_0^2}\left[\phi_\alpha^x(r)\phi_\alpha^x(r')\hat{x}\hat{x} + \phi_\alpha^y(r)\phi_\alpha^y(r')\hat{y}\hat{y} + \phi_\alpha^z(r)\phi_\alpha^z(r')\hat{z}\hat{z}\right]. \quad (3)$$

Equation (3), as well as (2), is a complete solution of the dyadic differential equation (1). It is valid both inside and outside of the source region. Although the singular nature of (3) or (2) in the source region is not immediately obvious, it can be shown numerically and it is in fact embedded in the irrotational, or the zero-curl, component of the dyad [5], [6]. Howard *et al.* [6] extracted the dominant singular term from the irrotational component of the dyad and showed that it has the same singularity as the free-space dyad. This will also become apparent in the next section when we reexpress the irrotational component of (3) into an image series using the Poisson summation transformation. Despite the singular nature in the source region, the dyad is valid in the sense that the singularity is integrable. For rigorous treatment on the singularity of the Green's function for a bounded region, we defer to the existing work, such as [7]–[9], available in the literature. In this paper, we will use the dyad as expressed in (3) with the implicit understanding that the function is to be treated as a distribution or a generalized function.

In computing the fields in a cavity, we resort to numerical computation. However, since the summation indices of (3) extend from 0 to ∞, numerical computation of $\overleftrightarrow{G}$ becomes more and more tedious as the observation point approaches the source point. This motivates our search for an alternate representation for the dyad which is more efficient from a computational viewpoint.

In searching for an alternate representation, our approach is to use the Poisson summation transformation to obtain a hybrid ray–mode representation for the dyad. This method of hybrid ray–mode reformulation is not new, being first developed for guided electromagnetic and acoustic fields [10]. For example in [11] and [12], the equivalence between mode and ray representations for guided propagation is illustrated. Treatment of waveguide fields using hybrid formulation can also be found in [13] and [14]. Different from the existing work cited above, our treatment is a reformulation for a three-dimensional cavity. We begin our treatment with a description and application of both the infinite and the finite Poisson summation transformation.

III. Infinite Poisson Transformation

A one-dimensional Poisson summation formula can be expressed as [15]

$$\sum_{n=-\infty}^{\infty} f(2n\pi) = \frac{1}{2\pi}\sum_{\nu=-\infty}^{\infty}\int_{-\infty}^{\infty} f(\tau)e^{i\nu\tau}\,d\tau \quad (4)$$

provided that $f(x)$ is a continuous function of x and $\sum_{n=-\infty}^{\infty} f(2n\pi)$ converges absolutely. Extending to three dimensions, we have

$$\sum\sum\sum_{m,n,p=-\infty}^{\infty} f(2m\pi, 2n\pi, 2p\pi) = \frac{1}{(2\pi)^3}\sum\sum\sum_{\alpha,\beta,\xi=-\infty}^{\infty}\int_{-\infty}^{\infty}\int_{-\infty}^{\infty}\int_{-\infty}^{\infty} f(\tau_1,\tau_2,\tau_3)\cdot e^{i(\alpha\tau_1+\beta\tau_2+\xi\tau_3)}\,d\tau_1\,d\tau_2\,d\tau_3. \quad (5)$$

The corresponding $f(m, n, p)$ in the dyadic Green's function expression (3) consists of different combinations of sin() and cos(). For illustrative purposes, we will consider only the case of a scalar Green's function similar in form to the different components embedded in $\overleftrightarrow{G}$. To generalize, a complex wavenumber $\tilde{k}_0$ will be used to represent the cavity medium.

Consider

$$G(r, r') = \sum\sum\sum_{m,n,p=0}^{\infty} \frac{\phi(r)\phi(r')}{\tilde{k}_0^2 - k_\alpha^2} = \frac{1}{8}\sum\sum\sum_{m,n,p=-\infty}^{\infty} \frac{\phi(r)\phi(r')}{\tilde{k}_0^2 - k_\alpha^2} \quad (6)$$

with

$$\phi(r) = \sin\left(\frac{m\pi}{a}x\right)\sin\left(\frac{n\pi}{b}y\right)\sin\left(\frac{p\pi}{c}z\right). \quad (6a)$$

By letting $k_x = m\pi/a$, $k_y = n\pi/b$, $k_z = p\pi/c$, and rewriting each sinusoid as exponentials, we can expand the product $\phi(r)\phi(r')$ into eight exponential terms, each in the form of $(\frac{1}{8}e^{\imath[k_xX+k_yY+k_zZ]})$, where $X = (x - x')$ or $(x + x')$, $Y = (y - y')$ or $(y + y')$, and $Z = (z - z')$ or $(z + z')$.

Consider each term separately in the generic form; let

$$f(m,n,p) = \frac{e^{\imath[k_xX+k_yY+k_zZ]}}{64\left(k_\alpha^2 - \tilde{k}_0^2\right)}. \quad (7)$$

If we apply the 3-D Poisson summation formula (5) to the summation of $f(m,n,p)$, the triple integration can be carried out in a straightforward manner by transforming to the spherical coordinates [16]. The result is

$$\sum_{m,n,p=0}^{\infty\infty\infty} f(m,n,p) = \frac{abc}{8}\sum_{\alpha,\beta,\xi=-\infty}^{\infty\infty\infty}\frac{e^{\imath\tilde{k}_0R(\alpha,\beta,\xi)}}{4\pi R(\alpha,\beta,\xi)} \quad (8)$$

where

$$R(\alpha,\beta,\xi) = \left[(X+2a\alpha)^2+(Y+2b\beta)^2+(Z+2c\xi)^2\right]^{1/2}.$$

Performing the similar transformation to every decomposed component of $\phi(r)\phi(r')$, we recombine and yield

$$\sum_{m,n,p=0}^{\infty\infty\infty}\frac{\phi(r)\phi(r')}{k_\alpha^2-\tilde{k}_0^2} = \frac{abc}{8}\sum_{\alpha,\beta,\xi=-\infty}^{\infty\infty\infty}\left\{\sum_{l=0}^{7}(-1)^l\frac{e^{\imath\tilde{k}_0R_l(\alpha,\beta,\xi)}}{4\pi R_l(\alpha,\beta,\xi)}\right\} \quad (9)$$

where

$$R_l = \left[(X_l+2a\alpha)^2+(Y_l+2b\beta)^2+(Z_l+2c\xi)^2\right]^{1/2} \quad (9a)$$

$$X_l = \begin{cases}(x-x'), & l=0,1,2,3\\ (x+x'), & l=4,5,6,7\end{cases};$$

$$Y_l = \begin{cases}(y-y'), & l=0,3,6,7\\ (y+y'), & l=1,2,4,5\end{cases};$$

$$Z_l = \begin{cases}(z-z'), & l=0,2,4,6\\ (z+z'), & l=1,3,5,7\end{cases}.$$

R_l represents the distance from the observation point to every image source. The right side of (9) is a summation of the free-space Green's function due to sources located at R_l. These sources correspond to the image sources resulting from the reflection at the cavity walls. Therefore, by the use of Poisson transformation we obtain an expression which has the physical interpretation of rays emanating from the various image sources. A result similar to (9) was obtained by Hamid *et al.* in [17]. Their approach was slightly different in that they started with the right side of (9) by invoking the image theorem. The Poisson summation formula was then applied to obtain a modal representation of the Green's function.

By reexpressing the modal sum into an image series, the singularity embedded in the modal sum becomes apparent. The modal sum on the left side of (9) comes from the irrotational component of the dyad in (2). The dominant singularity in the modal sum can be extracted easily from the image series and it is simply proportional to the $1/(4\pi R_0)$ term, where

$$R_0 = \left[(x-x')^2+(y-y')^2+(z-z')^2\right]^{1/2}.$$

This singularity agrees with the one obtained by Howard *et al.* in [6]. Moreover, it is consistent with the observation made by Lee *et al.* [8] that the dominant singular term in the Green's function for a bounded region is independent of the boundary.

IV. Finite Poisson Transformation

For finite sums over arbitrary intervals, the Poisson summation formula can be expressed as [18]

$$\sum_{l=n}^{N} f(l) = \sum_{\nu=-\infty}^{\infty}\int_{n+\alpha-1/2}^{N+\alpha+1/2} f(\tau)e^{\imath 2\nu\pi\tau}\,d\tau \quad (10)$$

where $f(x)$ is a function of real variable x such that $f(x)$ possesses a Fourier series expansion over any interval in the range $n-\alpha-1/2 < x < N+1-\alpha$. N and n are integers such that $n \leqslant N$, and α is any real number such that $|\alpha| < 1/2$.

For $\alpha = 0$, the summation formula in 3-D form can be expressed as

$$\sum_{m=m_0}^{M}\sum_{n=n_0}^{N}\sum_{p=p_0}^{P} f(m,n,p) = \sum_{\alpha,\beta,\xi=-\infty}^{\infty\infty\infty}\int_{m_0-1/2}^{M+1/2}\int_{n_0-1/2}^{N+1/2}\int_{p_0-1/2}^{P+1/2} f(\tau_1,\tau_2,\tau_3)\cdot e^{\imath 2\pi(\alpha\tau_1+\beta\tau_2+\xi\tau_3)}\,d\tau_1\,d\tau_2\,d\tau_3. \quad (11)$$

To apply (11) to the summation of the $f(m,n,p)$ defined in (7), we first transform the integration from rectangular coordinates to the spherical coordinates in a manner detailed in the Appendix. The justification for this involves the selection of a finite number of sets of (m,n,p) such that the corresponding value of k_α for each mode falls within a spherical shell of width $(k_2 - k_1)$, where $k_1 < k_0 < k_2$ (see Fig. 1). The integration volume on the right side of (11) is then approximated by the corresponding spherical shell. The result, as derived in the Appendix, is given as

$$\sum_{S_0}\sum\sum f(m,n,p) \approx \frac{abc}{8}\sum_{\alpha,\beta,\xi=-\infty}^{\infty\infty\infty}\frac{1}{8i\pi^2}g(\alpha,\beta,\xi;R) \quad (12)$$

where $g(\alpha,\beta,\xi;R)$ is defined in (A9); it consists of combinations of sine and cosine integral functions. The notation S_0 under the sums represents all the modes (m,n,p) such that $k_1 < k_\alpha < k_2$. This range is essentially a summation of all the modes near resonance.

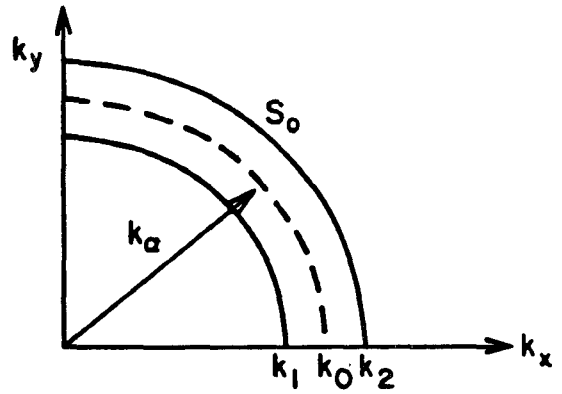

Fig. 1. A summation shell.

Performing the similar transformation to every decomposed component of $\phi(r)\phi(r')$ and combining with (9), we can express the Green's function as

$$\sum_{m=0}^{\infty}\sum_{n=0}^{\infty}\sum_{p=0}^{\infty}\frac{\phi(r)\phi(r')}{k_\alpha^2-\tilde{k}_0^2} \approx \sum_{S_0}\sum\sum\frac{\phi(r)\phi(r')}{k_\alpha^2-\tilde{k}_0^2}+\frac{abc}{8}\sum_{\alpha,\beta,\xi=-\infty}^{\infty}\sum\sum\sum_{l=0}^{7}(-1)^l \cdot\left\{\frac{e^{i\tilde{k}_0R_l}}{4\pi R_l}-\frac{1}{8\pi^2 i}g(\alpha,\beta,\xi;R_l)\right\} \quad (13)$$

where R_l, as given in (9a), is the distance from an observation point to an image source described by the parameters (α,β,ξ), and $g(\alpha,\beta,\xi;R_l)$ is defined in (A9) with R replaced by R_l. For ease of identification, we refer to the sum over S_0 as the mode sum, the second sum involving (α,β,ξ) as the ray sum, and the sum on the left side of (13) as the triple sum.

For the case of real k_0, if we choose S_0 to be symmetrical about k_0 so that $k_1=k_0-\gamma$, and $k_2=k_0+\gamma$, where 2γ is the summation shell width, then (13) can be simplified to

$$G(r,r')\approx\sum_{S_0}\sum\sum\frac{\phi(r)\phi(r')}{k_\alpha^2-k_0^2}+\frac{abc}{8}\sum_{\alpha,\beta,\xi=-\infty}^{\infty}\sum\sum\sum_{l=0}^{7}(-1)^l \cdot\left\{\frac{\cos(k_0R_l)}{4\pi R_l}\left(1-\frac{2}{\pi}\operatorname{Si}(\gamma R_l)\right)-\Delta_l\right\} \quad (14)$$

where

$$\Delta_l=\frac{\cos(k_0R_l)}{4\pi^2R_l}\left[\operatorname{Si}(R_l(2k_0+\gamma))-\operatorname{Si}(R_l(2k_0-\gamma))\right] -\frac{\sin(k_0R_l)}{4\pi^2R_l}\left[\operatorname{Ci}(R_l(2k_0+\gamma))-\operatorname{Ci}(R_l(2k_0-\gamma))\right]. \quad (14a)$$

For $\gamma \ll k_0$, Δ_l contributes only a negligible amount. When k_0R_l is small, the ray sum is dominated by $\cos(k_0R_l)/4\pi R_l$, and when γR_l is large, the image terms are oscillatory and are weighted by $(1/R_l^2\gamma)$.

A balancing effect exists between the mode sum and the ray sum. When we increase γ, i.e., increase the bandwidth for the mode sum, the number of modes that fall within the band will be increased. Therefore the contribution from the mode sum will be increased at the same time the quantity $(1-2/\pi\operatorname{Si}(R_l\gamma))$ decreases, thus reducing the contribution from the ray sum.

The hybrid representation of the Green's function as expressed in (14) is especially useful for cavities that are electrically large. When the dimensions of the cavity are large and the observation point is close to the source point (and away from the wall), the ray sum will be dominated by the self term, $\cos(k_0R_0)/4\pi R_0$, $R_0=[(x-x')^2+(y-y')^2+(z-z')^2]^{1/2}$. Therefore for a source located not near the wall, we can approximate (14) further to yield

$$\sum_{m=0}^{\infty}\sum_{n=0}^{\infty}\sum_{p=0}^{\infty}\frac{\phi(r)\phi(r')}{k_\alpha^2-k_0^2}\approx\sum_{S_0}\sum\sum\frac{\phi(r)\phi(r')}{k_\alpha^2-k_0^2} +\frac{abc}{8}\left[\frac{\cos(k_0R_0)}{4\pi R_0}\left(1-\frac{2}{\pi}\operatorname{Si}(\gamma R_0)\right)-\Delta_0\right] \quad (15)$$

where the correction

$$\Delta_0=\frac{\cos(k_0R_0)}{4\pi^2R_0}\left[\operatorname{Si}(R_0(2k_0+\gamma))-\operatorname{Si}(R_0(2k_0-\gamma))\right] -\frac{\sin(k_0R_0)}{4\pi^2R_0}\left[\operatorname{Ci}(R_0(2k_0+\gamma))-\operatorname{Ci}(R_0(2k_0-\gamma))\right] \quad (15a)$$

contributes a negligible amount. Numerical data showing the closeness of this approximation will be presented in the next section, along with the criterion for choosing a minimum γ.

Although (15) is only an approximation to the exact expression, addition of a few or more images will not necessarily improve the approximation in a monotonic fashion. This is so because while the higher order images are decaying at the rate of $1/R_l^2$, the number of images is increasing at the rate proportioned to R_l^2. Therefore the summation of the remaining terms is likely to be a slow but bounded oscillatory term of order $O(1)$. This contribution is negligible only because the mode sum usually has a large amplitude; i.e., $(k_\alpha^2-k_0^2)^{-1}\gg 1$ near resonance. As will be shown in the following numerical examples, retaining only those images with $k_0R_l \ll 1$ is sufficient to yield a satisfactory agreement with the numerically "exact" answer.

V. Numerical Examples

To simplify computations, we assume k_0 is real and the cavity is cubic. The frequency of operation is fixed at 1 GHz ($\lambda = 0.3$ m), and the length of the cavity is arbitrarily chosen to be $a=b=c=15.23\lambda$. Two cases will be considered. In case 1, we fix the source point near the center of the cavity and vary the observation distance. In case 2, we vary the source point along a vertical axis and show that

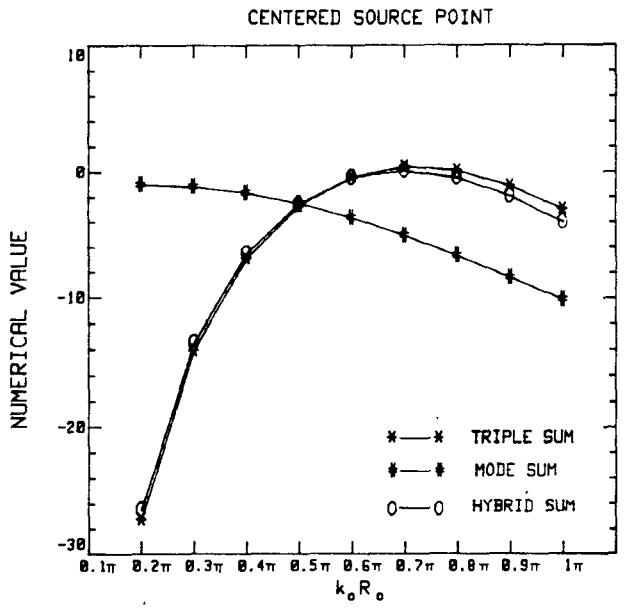

Fig. 2. Comparison of the mode sum and the hybrid sum with the triple sum for centered source point with $0.2\pi < k_0 R_0 < \pi$

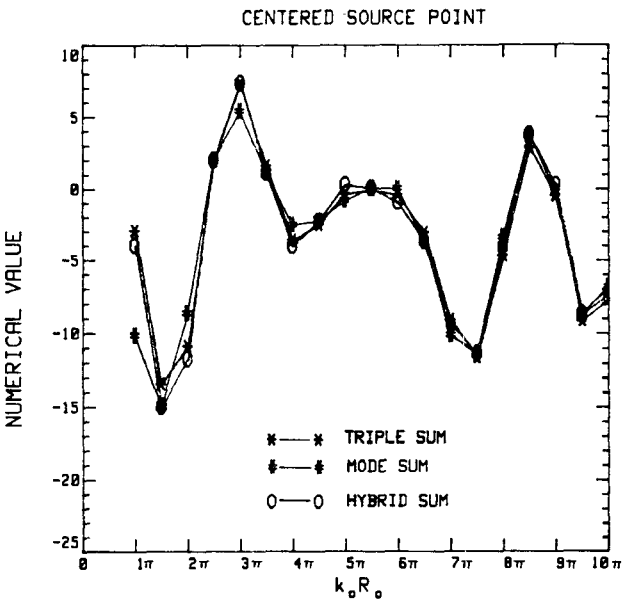

Fig. 3. Comparison of the mode sum and the hybrid sum with the triple sum for centered source point with $\pi < k_0 R_0 < 10\pi$.

when the source point is close to the ceiling, the first image must be included in (15) to get a good approximation.

In evaluating the triple sum, we first reduce $\sum_{m=0}^{\infty}\sum_{n=0}^{\infty}\sum_{p=0}^{\infty}\phi(r)\phi(r')/(k_\alpha^2 - k_0^2)$ to a double sum using a known summation result [19]. At the expense of long computation time, the reduced summations are summed with indices extending from 0 to a large number M. To minimize error, care is taken in the determination of M to ensure that the remaining sum from M to ∞ is negligible compared to the sum from 0 to M. Typically 90 000 terms are needed to yield an error of less than 1 percent for $k_0 R_0 \geq 0.15\pi$.

In what follows, we have chosen the half-width of the spherical shell to be $\gamma = 0.01 k_0$. This corresponds to a total of 831 "resonant modes" within the shell. As before, the term "triple sum" refers to the original unmodified triple summation, the term "mode sum" refers to the finite sum over all these resonant modes, and the term "hybrid sum" is the total contribution from the mode sum and the dominant term(s) of the ray sum.

Case 1: Centered Source Point

With the source point near the center, Fig. 2 shows the variations of the mode sum, the hybrid sum, and the triple sum with $k_0 R_0$ varying from 0.2π to π, and Fig. 3 has $k_0 R_0$ varying from π to 10π. R_0 is the distance between the source and the observation point. Within the range of small $k_0 R_0$, especially at $k_0 R_0 < \pi$, the self term plays an important role. With just the self term included, the hybrid sum provides a very good approximation to the triple modal sum.

As $k_0 R_0$ increases, the self term loses its dominant effect. At large $k_0 R_0$, i.e., $k_0 R_0 \geq 5\pi$, every term in the ray sum, including the self term, becomes very small. Therefore the contribution on the right side of (15) comes directly from the finite mode sum, as is evident in Fig. 3.

At the intermediate range of $k_0 R_0$ ($0.8\pi \leq k_0 R_0 \leq 2\pi$), the contribution from the self term is losing its dominant effect, but it is not quite small enough to be totally negligible. To further close the gap between the hybrid sum and the triple sum, we either have to sum all of the image terms or increase the bandwidth to increase the contribution due to the mode sum. However, a numerical check on the effect of increasing bandwidth showed that the computation time for the mode sum increases much faster than the convergence rate. Neither summing more images nor increasing the bandwidth appears to provide a viable way to close the gap, so we may have to accept the slight deviation from the exact value in exchange for fast computation time for $k_0 R_0$ in this intermediate range.

Case 2: Off-Centered Source Point

Figs. 4 and 5 show the variations of the mode sum, the hybrid sum, and the triple sum as the source point is varied. In this example, $k_0 R_0$ is fixed at 0.2π throughout, while $k_0 R_1$ is varied from 0.3π to 10π (see Fig. 6). With the first image term included, (15) becomes

$$\sum_{m,n,p=0}^{\infty}\sum\sum\sum \frac{\phi(r)\phi(r')}{k_\alpha^2 - k_0^2} \approx \sum_{S_0}\sum\sum \frac{\phi(r)\phi(r')}{k_\alpha^2 - k_0^2}$$

$$+ \frac{abc}{8}\sum_{l=0}^{1}(-1)^l\left[\frac{\cos(k_0 R_l)}{4\pi R_l}\left(1 - \frac{2}{\pi}\,\mathrm{Si}(\gamma R_l)\right) - \Delta_l\right] \quad (16)$$

where Δ_l is as defined in (14a), and

$$R_0 = \left[(x-x')^2 + (y-y')^2 + (z-z')^2\right]^{1/2},$$

$$R_1 = \left[(x-x')^2 + (y-y')^2 + (z-(2c-z'))^2\right]^{1/2}.$$

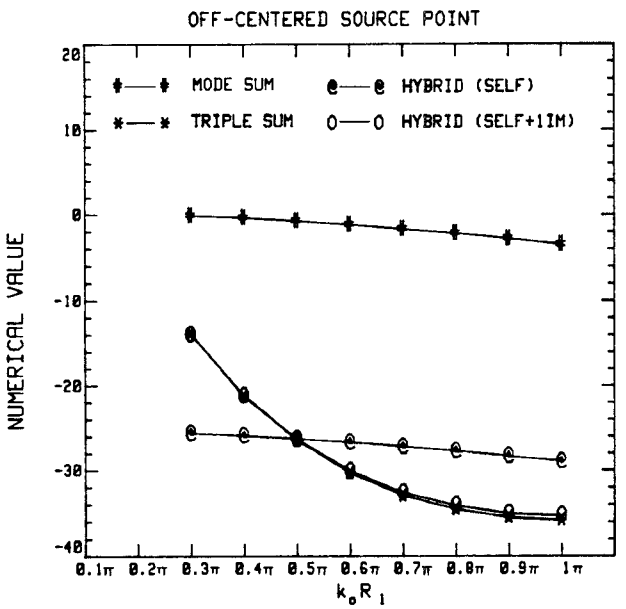

Fig. 4. Comparison of the mode sum and the hybrid sum with the triple sum for off-centered source point with $0.3\pi < k_0 R_1 < \pi$.

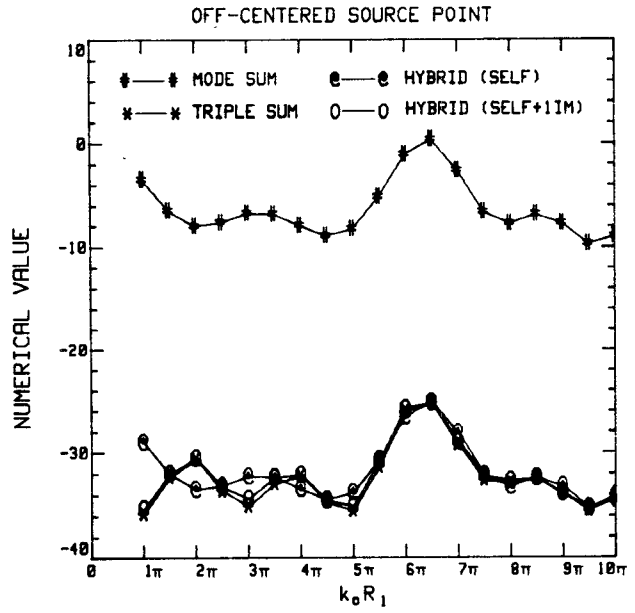

Fig. 5. Comparison of the mode sum and the hybrid sum with the triple sum for off-centered source point with $\pi < k_0 R_1 < 10\pi$.

When the source is close to the wall, i.e., when $k_0 R_1$ is small, the addition of the first image term becomes essential. Fig. 4 shows that without the addition of the first image term, the self term alone is not enough for the equality to hold in (15). As the source is moved away from the wall, i.e., $k_0 R_1$ is increased, Fig. 5 shows that the contribution from the first image in (16) becomes small (almost negligible at $k_0 R_1 \geq 6\pi$). With large $k_0 R_1$, we revert back to case 1, where the self term is dominant.

In the above calculations, we have chosen the half-width of the spherical shell, γ, to be $(0.01)k_0$. Increasing γ increases the number of modes in the band, which may

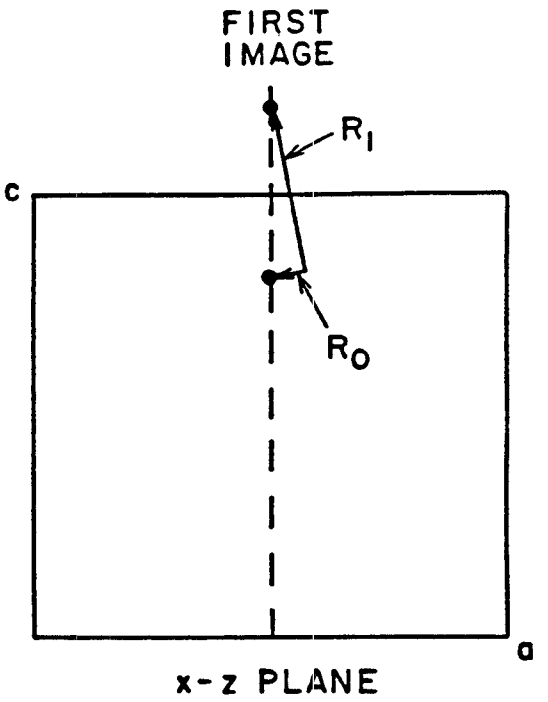

Fig. 6. A cross-sectional view of the first image distance R_1 and the distance R_0 between the source and the observation point.

increase the computation time if the number of modes in the mode sum is large. However, while decreasing the bandwidth may decrease the computation time, it may also introduce an approximation error which may cause (12) to become invalid if γ is too small. To show this we must go back to the derivation of (12) in the Appendix.

Fig. 9 displays the approximation we made in applying the finite Poisson transformation. The shaded grid area, which represents the range of integration for the function $F(\alpha, \beta, \xi)$ in (A3), is approximated by the spherical shell. Although we can arbitrarily choose the number of grids to match the shell, each grid has a minimum width since the minimum increment of (m, n, p) must be 1; i.e., the minimum summation interval must be from (m_0, n_0, p_0) to (m_0+1, n_0+1, p_0+1). The minimum grid width is therefore π/a, where a corresponds to the smallest dimension of the cavity. For our choice of $a = 15.23\lambda$ and $\gamma = 0.01k_0$, we have a ratio of shell width to minimum grid width of approximately 0.6, i.e.,

$$\text{width ratio} = \frac{2\gamma}{\pi/a} \approx 0.6. \tag{17}$$

To illustrate the effect of different shell widths, Fig. 7 shows the variation of the hybrid sum for $0.3\pi \leq k_0 R_0 \leq 0.4\pi$ as the width ratio is decreased below 0.6. With a very small width ratio, the deviation between the hybrid sum and the triple sum is indeed not acceptable. For width ratios greater than 0.6, we get into the region of slow convergence and increasing computation time. This trade-off does not seem to be worthwhile for choosing a width ratio greater than 0.6.

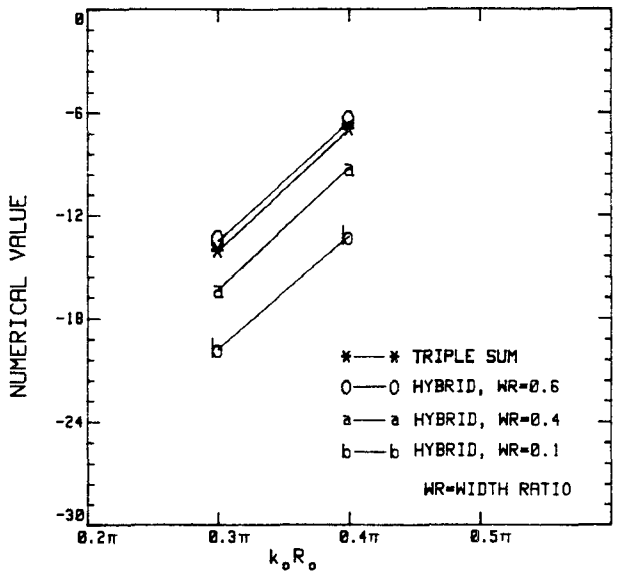

Fig. 7. Comparison of the hybrid sum with the triple sum for different width ratios.

VI. Summary

We have shown in this paper that the Green's function for a rectangular cavity in the modal form can be transformed into a hybrid representation consisting of a finite mode sum and a sum over all the images. This hybrid sum is effective for an electrically large cavity because it allows for the disposal of all the distance image terms without suffering an unacceptable loss of numerical accuracy. For r near r' and r' located away from the wall, a typical modal sum in the dyadic Green's function expression can be approximated as

$$\sum_{\alpha=(m,n,p)=0}^{\infty\sum\sum\sum} \frac{\phi(r)\phi(r')}{k_\alpha^2-k_0^2} \approx \sum_{S_0}\sum\sum\sum \frac{\phi(r)\phi(r')}{k_\alpha^2-k_0^2} + \frac{abc}{8}\left[\frac{\cos(k_0R_0)}{4\pi R_0}\left(1-\frac{2}{\pi}\,\mathrm{Si}(\gamma R_0)\right)\right]$$

where

$$\phi(r)=\sin\left(\frac{m\pi}{a}x\right)\sin\left(\frac{n\pi}{b}y\right)\sin\left(\frac{p\pi}{c}z\right)$$

$$R_0=\left[(x-x')^2+(y-y')^2+(z-z')^2\right]^{1/2}$$

and Si( ) is the sine integral function. The finite mode sum S_0 contains all the modes that fall within a preset summation bandwidth of 2γ centered about k_0. For an electrically large cavity, the selection of γ is arbitrary so long as it meets the criterion $\gamma \geq 0.3\ \pi/a$, where a is the smallest dimension of the cavity. When the source is close to the wall, the first image term must be included in the above equation to yield a good approximation (see (16)).

The hybrid representation developed in this paper is valid for either real or complex k_0. Except for the requirement that the bandwidth chosen for the mode sum not be too small, the hybrid representation is in general a good approximation of the modal representation, and it possesses unique properties that allow for feasible numerical evaluation. With this alternate representation, the effect of a scatterer in an electrically large rectangular cavity can be examined numerically. As illustrated in [20], this hybrid Green's function is most useful in the numerical computation of the induced current $\vec{J}$ and the scattered field for a simply structured scatterer in an electrically large rectangular cavity.

Appendix
Summing Over Finite Intervals

Consider the finite range sum defined as

$$Q=\sum_{m=m_0}^{M_0}\sum_{n=n_0}^{N_0}\sum_{p=p_0}^{P_0} f(m,n,p) = \sum_{m=m_0}^{M_0}\sum_{n=n_0}^{N_0}\sum_{p=p_0}^{P_0}\frac{e^{\imath(m\pi/aX+n\pi/bY+p\pi/cZ)}}{\left(k_\alpha^2-\tilde{k}_0^2\right)}. \quad \text{(A1)}$$

Applying the finite Poisson summation formula (11), and letting

$$k_x=\frac{\tau_1\pi}{a} \qquad k_y=\frac{\tau_2\pi}{b} \qquad k_z=\frac{\tau_3\pi}{c}$$

and

$$x_1=\left(m_0-\frac{1}{2}\right)\frac{\pi}{a} \qquad x_2=\left(M_0+\frac{1}{2}\right)\frac{\pi}{a} \qquad y_1=\left(n_0-\frac{1}{2}\right)\frac{\pi}{b}$$

$$y_2=\left(N_0+\frac{1}{2}\right)\frac{\pi}{b} \qquad z_1=\left(p_0-\frac{1}{2}\right)\frac{\pi}{c} \qquad z_2=\left(P_0+\frac{1}{2}\right)\frac{\pi}{c}$$

we can transform (A1) to

$$Q=\frac{abc}{\pi^3}\sum_{\alpha=-\infty}^{\infty}\sum_{\beta=-\infty}^{\infty}\sum_{\xi=-\infty}^{\infty} \cdot\int_{x_1}^{x_2}\int_{y_1}^{y_2}\int_{z_1}^{z_2} F(\alpha,\beta,\xi)\,dk_x\,dk_y\,dk_z \quad \text{(A2)}$$

where

$$F(\alpha,\beta,\xi)=\frac{e^{\imath[k_x(X+2a\alpha)+k_y(Y+2b\beta)+k_z(Z+2c\xi)]}}{\left(k_x^2+k_y^2+k_z^2\right)-\tilde{k}_0^2}. \quad \text{(A3)}$$

The summation intervals specified in (A1) transform directly into integration limits on the right side of (A2). A typical range of integration would correspond to the shaded area of Fig. 8, where each grid on the figure corresponds to a different set of summation interval (m_0, n_0, p_0) to (M_0, N_0, P_0). Suppose we now arbitrarily select a finite set of grids (or summation intervals) so that they are clustered around k_0 as shown in Fig. 9. Then

$$\left[\sum_{m_0}^{M_0}\sum_{n_0}^{N_0}\sum_{p_0}^{P_0}+\cdots+\sum_{m_l}^{M_l}\sum_{n_l}^{N_l}\sum_{p_l}^{P_l}\right]f(m,n,p) = \frac{abc}{\pi^3}\sum_{\alpha,\beta,\xi=-\infty}^{\infty}\left[\iiint_{\text{grid 1}}+\cdots+\iiint_{\text{grid }l}\right] \cdot F(\alpha,\beta,\xi)\,dk_x\,dk_y\,dk_z. \quad \text{(A4)}$$

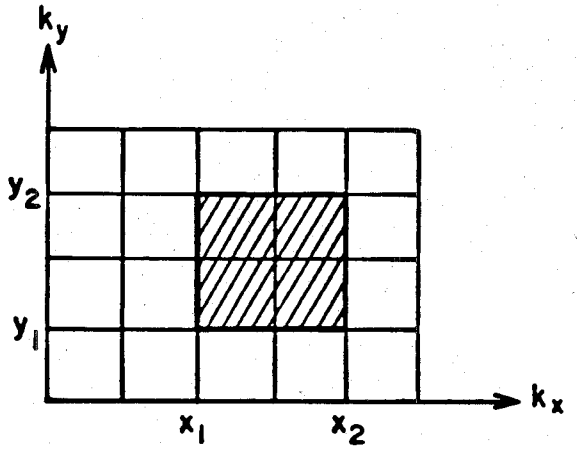

Fig. 8. A typical range of integration for the finite sum.

We now make the approximations

$$\left[\iiint_{\text{grid 1}} + \cdots + \iiint_{\text{grid } l}\right] F(\alpha,\beta,\xi)\, dk_x\, dk_y\, dk_z \approx \iiint_{V_0} F(\alpha,\beta,\xi)\, dk_x\, dk_y\, dk_z \quad \text{(A5)}$$

where V_0 is the volume of the spherical shell bounded by k_1 and k_2, and

$$\left[\sum_{m_0}^{M_0}\sum_{n_0}^{N_0}\sum_{p_0}^{P_0} + \cdots + \sum_{m_l}^{M_l}\sum_{n_l}^{N_l}\sum_{p_l}^{P_l}\right] f(m,n,p) \approx \sum\sum\sum_{S_0} f(m,n,p) \quad \text{(A6)}$$

where the S_0 represents all the modes (m, n, p) that fall within the spherical shell. Combining (A5) and (A6) above, we get

$$\sum\sum\sum_{S_0} f(m,n,p) \approx \frac{abc}{\pi^3} \sum\sum\sum_{\alpha,\beta,\xi=-\infty}^{\infty} \cdot \iiint_{V_0} \frac{e^{i[k_x(X+2a\alpha)+k_y(Y+2b\beta)+k_z(Z+2c\xi)]}}{\left(k_x^2+k_y^2+k_z^2\right)-\tilde{k}_0^2}\, dk_x\, dk_y\, dk_z. \quad \text{(A7)}$$

The triple integration of (A7) can be evaluated in a straightforward manner by transforming to the spherical coordinates using the following substitutions:

$$k^2 = k_x^2 + k_y^2 + k_z^2$$

$$k_x = k\sin\theta_k\cos\phi_k \qquad k_y = k\sin\theta_k\sin\phi_k \qquad k_z = k\cos\theta_k$$

$$\rho = \left[(X+2a\alpha)^2+(Y+2b\beta)^2\right]^{1/2}$$

$$R = \left[\rho^2+(Z+2c\xi)^2\right]^{1/2} \qquad \phi_{\alpha\beta} = \tan^{-1}\left(\frac{Y+2b\beta}{X+2a\alpha}\right).$$

The integrand becomes

$$F(\alpha,\beta,\xi) = \frac{e^{i\rho k\sin\theta_k\cos(\phi_k+\phi_{\alpha\beta})+ik\cos\theta_k(Z+2c\xi)}}{k^2-\tilde{k}_0^2}.$$

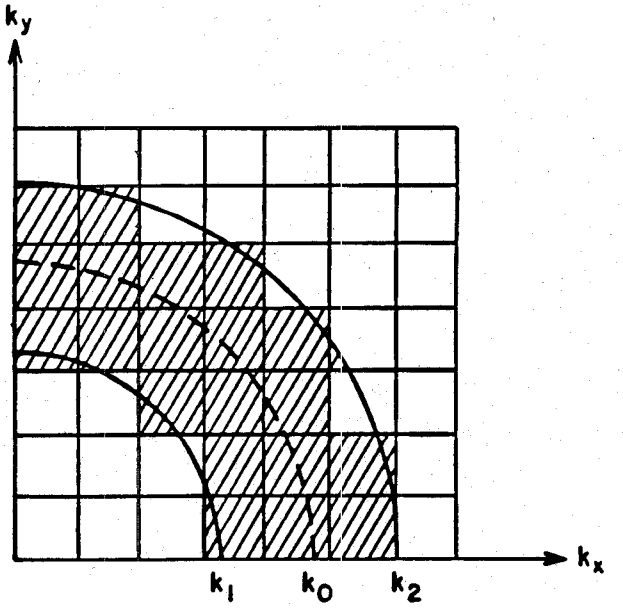

Fig. 9. Arrangement of a finite set of summation intervals.

The result of this integration is

$$\sum\sum\sum_{S_0} f(m,n,p) \approx \frac{abc}{i\pi^2} \sum\sum\sum_{\alpha,\beta,\xi=-\infty}^{\infty} g(\alpha,\beta,\xi;R) \quad \text{(A8)}$$

where

$$\begin{aligned} g(\alpha,\beta,\xi;R) = {} & \frac{2\cos(\tilde{k}_0R)}{iR}\left[\mathrm{Si}\left(R\left(\tilde{k}_0-k_2\right)\right)\right. \\ & -\mathrm{Si}\left(R\left(\tilde{k}_0-k_1\right)\right)+\mathrm{Si}\left(R\left(\tilde{k}_0+k_1\right)\right) \\ & \left.-\mathrm{Si}\left(R\left(\tilde{k}_0+k_2\right)\right)\right] \\ & +\frac{2\sin(\tilde{k}_0R)}{iR}\left[\mathrm{Ci}\left(R\left(\tilde{k}_0-k_1\right)\right)\right. \\ & -\mathrm{Ci}\left(R\left(\tilde{k}_0-k_2\right)\right)-\mathrm{Ci}\left(R\left(\tilde{k}_0+k_1\right)\right) \\ & \left.+\mathrm{Ci}\left(R\left(\tilde{k}_0+k_2\right)\right)\right]. \end{aligned} \quad \text{(A9)}$$

Si and Ci are the sine and cosine integrals, defined as $\mathrm{Si}(z) = \int_0^z \sin t/t\, dt$, and $\mathrm{Ci}(z) = -\int_z^\infty \cos t/t\, dt$. For real k_0 and a symmetrical shell width, i.e., $k_1 = k_0 - \gamma$, $k_2 = k_0 + \gamma$, (A9) reduces to

$$\begin{aligned} g(\alpha,\beta,\xi;R) = {} & \frac{2\cos(k_0R)}{iR}\left[-2\,\mathrm{Si}(R\gamma)+\mathrm{Si}\left(R(2k_0-\gamma)\right)\right. \\ & \left.-\mathrm{Si}\left(R(2k_0+\gamma)\right)\right] \\ & +\frac{2\sin(k_0R)}{iR}\left[-i\pi-\mathrm{Ci}\left(R(2k_0-\gamma)\right)\right. \\ & \left.+\mathrm{Ci}\left(R(2k_0+\gamma)\right)\right]. \end{aligned} \quad \text{(A10)}$$

REFERENCES

[1] P. Corona, G. Latmiral, E. Paolini, and L. Piccioli, "Use of a reverberating enclosure for measurements of radiated power in the microwave range," *IEEE Trans. Electromagn. Compat.*, vol. EMC-22, pp. 54–59, 1976.

[2] B. H. Liu, D. C. Chang, and M. T. Ma, "Eigenmodes and the composite quality factor of a reverberating chamber," Nat. Bur. Stand. (U.S.), NBS Tech. Note 1066, Aug. 1983.

[3] Y. Rahmat-Samii, "On the question of computation of the dyadic Green's function at the source region in waveguides and cavities," *IEEE Trans. Microwave Theory Tech.*, vol. MTT-23, pp. 762–765, 1975.
[4] C. T. Tai and P. Rozenfeld, "Different representations of dyadic Green's functions for a rectangular cavity," *IEEE Trans. Microwave Theory Tech.*, vol. MTT-24, pp. 597–601, 1976.
[5] W. A. Johnson, A. Q. Howard, and D. G. Dudley, "On the irrotational component of the electric Green's dyadic," *Radio Sci.*, vol. 14, pp. 961–967, Nov. 1979.
[6] A. Q. Howard, and D. B. Seidel, "Singularity extraction in kernel functions in closed region problems," *Radio Sci.*, vol. 13, pp. 425–429, May 1978.
[7] A. D. Yaghjian, "Electric dyadic Green's functions in the source region," *Proc. IEEE*, vol. 68, pp. 248–263, Feb. 1980.
[8] S. W. Lee, J. Boersma, C. L. Law, and G. A. Deschamps, "Singularity in Green's function and its numerical evaluation," *IEEE Trans. Antennas Propagat.*, vol. AP-28, pp. 311–317, May 1980.
[9] J. J. H. Wang, "A unified and consistent view on the singularities of the electric dyadic Green's function in the source region," *IEEE Trans. Antennas Propagat.*, vol. AP-30, pp. 463–468, May 1982.
[10] L. B. Felsen, *Hybrid Formulation of Wave Propagation and Scattering*. Dordrecht, Holland: Martinus Nijhoff, 1984, pp. 3–21.
[11] T. F. Gao and E. C. Shang, "The transformation between the mode representation and the generalized ray representation of a sound field," *J. Sound Vib.*, vol. 80, pp. 105–115, 1982.
[12] A. Kamel and L. B. Felsen, "On the ray equivalent of a group of modes," *J. Acoust. Soc. Amer.*, vol. 71, pp. 1447–1452, 1982.
[13] L. B. Felsen and A. Kamel, "Hybrid ray-mode formulation of parallel waveguide Green's functions," *IEEE Trans. Antennas Propagat.*, vol. AP-29, pp. 637–649, 1981.
[14] T. Ishihara, L. B. Felsen, and A. Green, "High-frequency fields excited by a line source on a perfectly conducting concave cylindrical surface," *IEEE Trans. Antennas Propagat.*, vol. AP-26, pp. 757–767, 1978.
[15] R. Courant and D. Hilbert, *Methods of Mathematical Physics* vol. 1. New York: Interscience, 1962.
[16] D. I. Wu and D. C. Chang, "An investigation of a ray-mode representation of the Green's function in a rectangular cavity," Nat. Bur. Stand. (U.S.), NBS Tech. Note 1312, Sept. 1987.
[17] M. A. K. Hamid and W. A. Johnson, "Ray-optical solution for the dyadic Green's function in a rectangular cavity," *Electron. Lett.*, vol. 6, pp. 317–319, May 1970.
[18] B. J. B. Crowley, "Some generalization of the poisson summation formula," *J. Phys. A: Math. Gen.*, vol. 12, pp. 1951–1955, 1979.
[19] R. E. Collin, *Field Theory of Guided Waves*. New York: McGraw-Hill, 1960.
[20] D. I. Wu, "On the effect of a rotating scatterer in an over-moded rectangular cavity," Ph.D. dissertation, Univ. of Colorado, Boulder, May 1987.

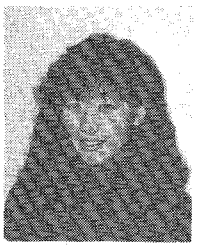

Doris I. Wu (S'78–S'85–M'87) was born on February, 26, 1958. She received the B.S. degree from Michigan State University, East Lansing, in 1980, the M.S. degree from Stanford University, Stanford, Ca, in 1981, and the Ph.D. degree in 1987 from the University of Colorado, Boulder, all in electrical engineering.

From 1980 to 1983 she was a Member of Technical Staff at Bell Laboratories/AT&T, Indianapolis, IN where she was engaged in the study of radio frequency interference. In 1987 she joined the research staff at the Electromagnetic Fields Division of the National Bureau of Standards in Boulder, CO. Her current research interests include wave propagation, antenna radiation, scattering, and numerical modeling.

✠

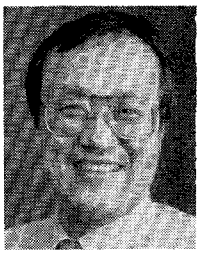

David C. Chang (S'65–M'67–SM'76–F'85) received the Ph.D. degree in applied physics from Harvard University, Cambridge, MA, in 1967.

He joined the faculty in the Department of Electrical and Computer Engineering, University of Colorado, Boulder, in September 1967 and has been a Professor of Electrical and Computer Engineering since 1975 and Chairman of the Department since 1982. He is also currently the Director for the NSF Industry/University Cooperative Research Center for Microwave/Millimeter-Wave Computer-Aided Design at the University of Colorado. He has been active in electromagnetic theory, antennas and microwave circuits research.

Dr. Chang has served, on various occasions, as the Associate Editor (1980–82), coordinator for the Distinguished Lecturers Program (1982–85), Chair of the Ad Hoc Committee for Basic Research (1985–88), and a member of the Administrative Committee (1985–present) of the IEEE Professional Society on Antennas and Propagation; as a member of the Technical Subcommittee on Microwave Field Theory of the IEEE Professional Society on Microwave Theory and Techniques (1975–85); as a member-at-large (1982–85) and Secretary of the U.S. National Committee (1982–85), as well as Chair of the Technical Program Committee, Commission B on Fields and Waves (1983–86) of the International Union of Radio Science.